Communications in Theoretical Physics

Commun. Theor. Phys. **78** (2026) 025603 (9pp) https://doi.org/10.1088/1572-9494/ae088b
CSTR: 32041.14.CTPae088b

Thermal properties of the Dirac oscillator in Amelino-Camelia and Magueijo-Smolin DSR theories

Abdelmalek Boumali[1,*] **and Nosratollah Jafari**[2,3,4]

[1] Laboratory of Theoretical and Applied Physics, Echahid Cheikh Larbi Tebessi University, Algeria
[2] Fesenkov Astrophysical Institute, 050020 Almaty, Kazakhstan
[3] Al-Farabi Kazakh National University, Al-Farabi av. 71, 050040 Almaty, Kazakhstan
[4] Center for Theoretical Physics, Khazar University, 41 Mehseti Street, Baku AZ1096, Azerbaijan

E-mail: abdelmalek.boumali@univ-tebessa.dz, boumali.abdelmalek@gmail.com and nosrat.jafari@fai.kz

Received 18 July 2025, revised 30 August 2025
Accepted for publication 18 September 2025
Published 23 October 2025

Abstract

This study investigates the thermal and statistical properties of the Dirac oscillator within the framework of two prominent formulations of doubly special relativity (DSR): the Amelino-Camelia and Magueijo-Smolin models. DSR extends Einstein's special relativity by introducing an additional invariant scale—the Planck energy—leading to modified energy-momentum relations that encode potential quantum-gravitational effects at ultra-high energies. In this context, we derive the modified Dirac equations for both DSR scenarios and analytically determine the corresponding energy spectra. These spectra are subsequently used to compute the partition function and key thermodynamic quantities, including specific heat, by employing the Euler–Maclaurin formula to facilitate an efficient approximation of the partition function. The analysis is restricted to the positive-energy sector, enabled by the exact Foldy–Wouthuysen transformation, which effectively decouples positive and negative energy states. The findings reveal that Planck-scale deformation parameters induce significant modifications in the energy spectrum and thermodynamic behavior of the Dirac oscillator in each DSR framework, thereby offering valuable insights into possible observable imprints of quantum gravitational phenomena in relativistic quantum systems.

Keywords: Dirac oscillator, thermal properties, Amelino–Camelia and Magueijo–Smolin DSR theories

(Some figures may appear in colour only in the online journal)

1. Introduction

In the relativistic extension known as the Dirac oscillator, the canonical momentum $\overrightarrow{p}$ in the Dirac equation, is substituted with $\overrightarrow{p} - im\gamma^0\omega\overrightarrow{r}$, a modification first proposed by Ito *et al* [1]. Moshinsky and Szczepaniak subsequently introduced the term 'Dirac oscillator' (DO) and showed that, in the non-relativistic limit, it simplifies to a harmonic oscillator integrated with a significant spin–orbit interaction [2]. The DO interaction can be comprehended as a coupling of an anomalous magnetic moment to a linearly growing electric field, with the corresponding electromagnetic potential explicitly determined by Benitez *et al* [3]. The precise solutions of the DO and its extensive applications—from particle phenomenology to quantum optics [4–7]—have been widely studied. The initial experimental demonstration, conducted in a one-dimensional microwave resonator by Franco-Villafane *et al* [8], led to further studies on Dirac oscillators by the authors [6, 9–14].

DSR improves Einstein's special relativity by incorporating an additional invariant scale: the Planck energy $E_p = \sqrt{\hbar c^5/G} \approx 10^{19}$ GeV, in conjunction with the invariant speed of light c. Conventional special relativity maintains the invariance of c, but deformed special relativity alters the energy-momentum relations to include hypothetical

* Author to whom any correspondence should be addressed.

quantum-gravitational phenomena that emerge at ultrahigh energies. Two fundamental DSR models are the Amelino-Camelia proposal [15, 16] and the Magueijo-Smolin (MS) framework [17]. Additionally, a new projective formalism of the MS DSR is presented in [18]. These theories examine Planck-scale physics, with relativistic oscillators such as DO to investigate the intersection of quantum mechanics and gravity [18–23].

These frameworks provide essential phenomenological tools for examining the impact of Planck-scale alterations on fundamental quantum systems [18–23]. Relativistic quantum oscillators, exemplified by the Dirac oscillator, serve as optimal theoretical frameworks for examining the interaction between quantum mechanics, relativistic principles, and gravity-induced modifications. Comprehending the impact of DSR-induced deformations on the energy spectra and thermodynamic properties of the DO can provide crucial insights into quantum gravity phenomenology and assist in detecting experimental signals at high-energy scales.

This research investigates the thermal and statistical properties of the one-dimensional Dirac oscillator within the Amelino-Camelia and MS DSR theories. We derive the modified Dirac equations and solve them to obtain their energy spectra, enabling us to calculate partition functions and essential thermodynamic parameters, including specific heat. The analysis highlights the impact of Planck-scale deformation parameters on system behavior, specifically on the positive energy solutions derived from the Foldy–Wouthuysen transformation.

The document is structured as follows: section 2 elucidates the origin and resolution of the Dirac oscillator within the framework of the MS DSR model. Section 3 employs a comparable methodology within the Amelino-Camelia framework, obtaining the associated updated oscillator equations and energy spectra. Section 4 analyzes the statistical and thermodynamic characteristics, offering analytical approximations for the partition function and specific heat in both DSR contexts. Ultimately, section 5 encapsulates the key findings and delineates avenues for future research.

2. The modified Dirac oscillator in MS DSR theory

In the MS DSR framework, the modified Dirac equation of order $O(E^2/E_p^2)$ is given by

$$\left[\mathrm{i}\gamma^{\mu}\partial_{\mu} - m\left(1 - \frac{\mathrm{i}}{E_p}\partial_t\right)\right]\tilde{\psi} = 0. \tag{1}$$

For the Dirac oscillator, this becomes

$$\{\alpha_x(p_x - \mathrm{i}m\omega\gamma^0 x) + \gamma^0 M\}\psi_D = E\psi_D, \tag{2}$$

where $M = m\left(1 - \frac{\mathrm{i}}{k}\partial_t\right)$, $\psi_D = (\psi_1, \psi_2)^{\mathrm{T}}$, $\alpha_x = \sigma_x$, and $\gamma^0 = \sigma_z$.

This leads to the equation

$$\left(\frac{p_x^2}{2m} + \frac{m\omega^2}{2}x^2\right)\psi_1(x) = \tilde{E}\psi_1(x), \tag{3}$$

with the energy relation

$$\frac{m\omega + E^2 - m^2\left(1 - \frac{E}{E_p}\right)^2}{2m} = \omega\left(n + \frac{1}{2}\right). \tag{4}$$

Solving for E, the energy eigenvalues are

$$E = -\frac{m^2 E_p}{E_p^2 - m^2} \pm \frac{E_p m\sqrt{E_p^2 + 2E_p^2 n\frac{\omega}{m} - 2\,mn\omega}}{E_p^2 - m^2}. \tag{5}$$

As $E_p \to \infty$, this reduces to the standard Dirac oscillator spectrum [6]

$$E = \pm m\sqrt{1 + 2n\frac{\omega}{m}}. \tag{6}$$

3. The modified Dirac oscillator in Amelino–Camelia DSR theory

In the Amelino-Camelia DSR framework, the modified Dirac equation to order $O(E^2/E_p^2)$ is

$$\left[i\gamma^0\partial_0 + i\gamma^i\partial_i\left(1 + \frac{\mathrm{i}}{2E_p}\partial_t\right) - m\right]\tilde{\psi} = 0. \tag{7}$$

For the Dirac oscillator, this leads to

$$\alpha_x(p_x - \mathrm{i}m\omega\gamma^0 x)\psi_D = \left(\frac{E - m\gamma^0}{1 + \frac{E}{2E_p}}\right)\psi_D. \tag{8}$$

The resulting equation for the upper component is

$$\left(\frac{p_x^2}{2m} + \frac{m\omega^2}{2}x^2\right)\psi_1(x) = \left(\frac{\omega}{2} + \frac{E^2 - m^2}{2\,m\left(1 + \frac{E}{2E_p}\right)^2}\right)\psi_1(x). \tag{9}$$

The energy quantization condition becomes

$$\frac{\omega}{2} + \frac{E^2 - m^2}{2\,m\left(1 + \frac{E}{E_p}\right)^2} = \omega\left(n + \frac{1}{2}\right). \tag{10}$$

Solving for E, the energy eigenvalues are

$$E_{\pm} = \frac{2E_p mn\omega}{2E_p^2 - mn\omega} \pm \frac{2E_p^2\sqrt{m^2 + 2\,mn\omega - \frac{m^3 n\omega}{2E_p^2}}}{2E_p^2 - mn\omega}. \tag{11}$$

As $E_p \to \infty$, this reduces to the standard Dirac oscillator result

$$E_{\pm}(n) = \pm\sqrt{m^2 + 2nm\omega}. \tag{12}$$

This shows how the energy spectrum depends on the quantum number n and the deformation parameter E_p, recovering the usual result in the undeformed limit [6].

4. Statistical properties

We summarize the key results from the previous section.

- Equations (5) and (11) serve as the foundational expressions to evaluate thermodynamic quantities such as the partition function and the specific heat of the oscillator.
- The differences between these equations offer, in principle, observable signatures that could distinguish various quantum gravity-inspired modifications of special relativity, as explored further through the analysis and figures presented in this work.

In essence, equations (5) and (11) respectively represent the fundamental energy spectra for the one-dimensional Dirac oscillator in two well-known DSR models. They demonstrate how Planck-scale effects impact quantum systems, in which case different DSR models lead to distinct possible shifts in the energy levels and, consequently, different thermodynamic predictions.

Our primary goal in this section is to determine the statistical properties of the system, with a particular emphasis on calculating the partition function Z. Inspired from [6, 24–26], we define the partition function as:

$$Z = 1 + \sum_{n=1}^{\infty} \mathrm{e}^{-\beta E_n}. \tag{13}$$

Although conceptually the expansion should be written as an infinite series, numerical evaluations of the series can be problematic or impossible for complex systems. To circumvent this situation, we employ the Euler–Maclaurin formula —an analytical method extensively described in the literature (see [27]). This formula interpolates between discrete sums and continuous integrals, allowing integrals to estimate sums plus correction terms expressed in terms of derivatives, Bernoulli polynomials, and/or constants.

The Euler–Maclaurin formula in full generality is written as [27]

$$\begin{aligned}\sum_{n=a}^{b} f(n) = {} & \frac{f(b)+f(a)}{2} + \int_a^b f(n)\mathrm{d}n \\ & + \sum_{i=2}^{p} \frac{B_i}{i!}\left(f^{(i-1)}(b) - f^{(i-1)}(a)\right) \\ & - \int_a^b \frac{\bar{B}_p(t)}{p!} f^{(p)}(t)\mathrm{d}t,\end{aligned} \tag{14}$$

where a and b are integers numbers; $b - a$ is an integer; B_n are Bernoulli numbers; B_p are Bernoulli polynomials; and p is a positive integer. The function f is assumed to have continuous pth-order derivatives. Where the remainder term is referred to as

$$R_k = \int_a^b \frac{B_p(1-t)}{p!} f^{(p)}(t)\mathrm{d}t. \tag{15}$$

In our case

$$f(n) = \mathrm{e}^{-\frac{\beta}{2E_p^2 - mn\omega}\left(2E_p\, mn\omega + 2E_p^2\sqrt{m^2 + 2mn\omega - \frac{m^3 n\omega}{2E_p^2}}\right)}. \tag{16}$$

It is powerful in providing a good approximation to the function, particularly when $f(n)$ and its derivatives decrease rapidly as n increases. When $f(n)$ and all its derivatives vanish at infinity, the formula becomes (see [13])

$$\begin{aligned}\sum_{n=0}^{\infty} f(n) = {} & \frac{f(0)}{2} + \int_0^{\infty} f(n)\,\mathrm{d}n + \sum_{i=2}^{p} \frac{B_i}{i!} f^{(i-1)}(0) \\ & - \int_0^{\infty} \frac{\bar{B}_p(\{t\})}{p!} f^{(p)}(t)\,\mathrm{d}t.\end{aligned} \tag{17}$$

The first few Bernoulli numbers are $B_0 = 1$, $B_1 = -\frac{1}{2}$, $B_2 = \frac{1}{6}$ and $B_4 = -\frac{1}{30}$, and all Bernoulli numbers B_k are 0 for all odd $k > 1$. Bernoulli polynomials $B_n(x)$ can be characterized using a generating function

$$\frac{t\mathrm{e}^{tx}}{\mathrm{e}^t - 1} = \sum_{n=0}^{\infty} B_n(x)\frac{t^n}{n!}, \tag{18}$$

with the first few polynomials

$$\begin{aligned} B_0(x) &= 1, \\ B_1(x) &= x - \frac{1}{2}, \\ B_2(x) &= x^2 - x + \frac{1}{6}, \\ B_3(x) &= x^3 - \frac{3}{2}x^2 + \frac{1}{2}x. \end{aligned} \tag{19}$$

In contrast to classical Bernoulli polynomials, periodic Bernoulli functions, denoted by $\bar{B}_p(\cdot)$, are defined explicitly in terms of the fractional part of their arguments. Specifically, they satisfy

$$\bar{B}_p(x) = B_p(x - \lfloor x \rfloor), \quad x \in \mathbb{R}, \tag{20}$$

where the fractional part $\{x\}$ is defined by

$$x = x - \lfloor x \rfloor, \quad 0 \leqslant x < 1. \tag{21}$$

Consequently, the periodic Bernoulli function $\bar{B}_p(\{x\})$ exhibits exact periodicity with a period of unity. This feature distinctly differentiates it from the polynomial form $B_p(x)$, which displays polynomial growth without periodicity. Another essential characteristic of periodic Bernoulli functions is their piecewise smooth structure. Discontinuities may occur at integer points $x \in \mathbb{Z}$, except for the trivial case $p = 0$. In contrast, classical Bernoulli polynomials are infinitely differentiable and continuous over the entire real axis. Furthermore, a fundamental property distinguishing periodic Bernoulli functions is that their integral over one complete period vanishes

$$\int_0^1 \bar{B}_p(x)\,\mathrm{d}x = 0, \quad p \geqslant 1. \tag{22}$$

Periodic Bernoulli functions naturally appear within the Euler–Maclaurin summation formula, where they provide accurate remainder estimations for numerical series

expansions. Their periodic and oscillatory characteristics yield concise and rigorous descriptions of subtle corrections needed when transitioning between discrete sums and continuous integrals.

The Euler–Maclaurin formula demonstrates considerable utility in this context, as illustrated in [13, 14]. By converting discrete sums into integrals supplemented by systematic correction terms, this methodology provides enhanced analytical clarity and improved computational efficiency. Frequently, the principal integral component can either be evaluated explicitly or calculated efficiently using numerical methods. Concurrently, the series of correction terms—originating from higher-order derivatives and Bernoulli numbers or polynomials—progressively refines the precision of the resultant approximation. An essential feature of this framework is the integral role played by the periodic Bernoulli function within the remainder term. This incorporation extends beyond mere technicality, serving as a rigorous and succinct representation of the inherent oscillatory behavior inherent to discrete summations—behavior that integral and polynomial corrections alone fail to capture adequately. This inclusion substantially enhances both convergence characteristics and the accuracy of approximations, especially in cases involving slowly convergent or highly oscillatory series. Consequently, the periodic Bernoulli function is indispensable for accurately quantifying residual fluctuations, providing refined control over error estimation and significantly contributing to the overall reliability of the method. These attributes render the Euler–Maclaurin approach particularly effective for evaluating partition functions and analogous summations, where direct numerical computation may prove impractical or computationally demanding. When augmented by the periodic Bernoulli remainder term, the Euler–Maclaurin formula constitutes a robust and systematic framework for extracting asymptotic expansions and establishing rigorous error bounds. This synthesis ensures high-precision quantitative outcomes while optimizing computational resources. Ultimately, the Euler–Maclaurin formula's enduring significance in mathematical and physical analyses derives from its harmonious balance of analytical rigor and practical effectiveness, notably enhanced by the inclusion of periodic Bernoulli functions.

In our case, for any positive integer n, the periodic Bernoulli function $\bar{B}_n$ is defined as $\bar{B}_n = B_n(\{x\})$, where $\{x\}$ is the fractional part of x. This function is periodic with period 1 and continuous over it, a property which, combined with Elliott's result [28], yields the ultimate form of the partition function sum [13, 14]

$$\sum_{n=0}^{\infty} f(n) = \frac{f(0)}{2} + \int_0^{\infty} f(n)\mathrm{d}n + \sum_{i=2}^{p} \frac{B_i f^{(i-1)}(0)}{i!} - \int_0^1 \frac{\bar{B}_p(\{t\})}{p!} f^{(p)}(t)\mathrm{d}t. \tag{23}$$

Within statistical physics, numerous thermodynamic quantities—including the partition function $Z(\beta)$, free energy $F(\beta)$, internal energy $U(\beta)$, entropy $S(\beta)$, and specific heat $C_v(\beta)$—can be systematically derived from the Boltzmann factor $\mathrm{e}^{-\beta E}$. These quantities illuminate the macroscopic properties of a system grounded in its microscopic energy structure. Their relationships to the partition function are

$$F(\beta) = -\frac{1}{\beta}\ln Z(\beta), \quad U(\beta) = -\frac{\partial \ln Z(\beta)}{\partial \beta}, \quad \frac{S(\beta)}{k_{\mathrm{B}}} = \ln Z(\beta) - \beta\frac{\partial \ln Z(\beta)}{\partial \beta}, \quad \frac{C_{\mathrm{V}}(\beta)}{k_{\mathrm{B}}} = \beta^2\frac{\partial^2 \ln Z(\beta)}{\partial \beta^2}, \tag{24}$$

where $\beta = 1/(k_{\mathrm{B}}T)$, with k_{B} being Boltzmann's constant and T the absolute temperature. The partition function $Z(\beta)$ encapsulates the statistical weights of all accessible energy states and fundamentally governs the thermodynamic behavior.

Note that the specific heat C_{V} includes the subscript v to indicate that the derivative concerning temperature is evaluated at constant V, which represents length (one-dimensional systems), area (two-dimensional systems), or volume (three-dimensional systems), depending on the dimensionality of the system under consideration. This distinction is important, as the physical interpretation of C_{V} inherently depends upon the geometry and constraints of the given system. Moreover, within the Amelino-Camelia (AC) Doubly Special Relativity (DSR) framework, the energy spectrum is subject to an upper bound given by $n_c = 2[E_p]^2$, where $[E_p]$ denotes the integer part of E_p. Consequently, the Euler–Maclaurin expansion (initially presented as equation (26)) must be adjusted to account explicitly for this finite summation range. In contrast, under the Magueijo-Smolin (MS) prescription, the standard infinite-range form of the Euler–Maclaurin expansion remains valid.

$$\sum_{n=0}^{\infty} f(n) = \frac{f(0)}{2} + \int_0^{\infty} f(n)\mathrm{d}n + \sum_{i=2}^{p} \frac{B_i f^{(i-1)}(0)}{i!} - \int_0^1 \frac{\bar{B}_p(t)}{p!} f^{(p)}(t)\mathrm{d}t, \tag{25}$$

whereas in the AC case the integral is truncated at the maximal level $n_c = 2[E]_p^2$

$$\sum_{n=0}^{n_c} f(n) = \frac{f(0)}{2} + \int_0^{[E_p]^2} f(n)\mathrm{d}n + \sum_{i=2}^{p} \frac{B_i f^{(i-1)}(0)}{i!} - \int_0^1 \bar{B}_p(t)\,\frac{f^{(p)}(t)}{p!}\mathrm{d}t. \tag{26}$$

Here, the fractional part x is given explicitly by: $t = t - [t]$, 7D10 $\leqslant t < 1$.

The upper limit $[E_p]^2$ reflects the fact that, in the AC DSR theory, quantum levels are only defined for $n \in [0, 2[E_p]^2]$.

Such thermodynamic quantities not only characterize equilibrium properties, but are also at the foundation of a description of phase transitions, response functions, and

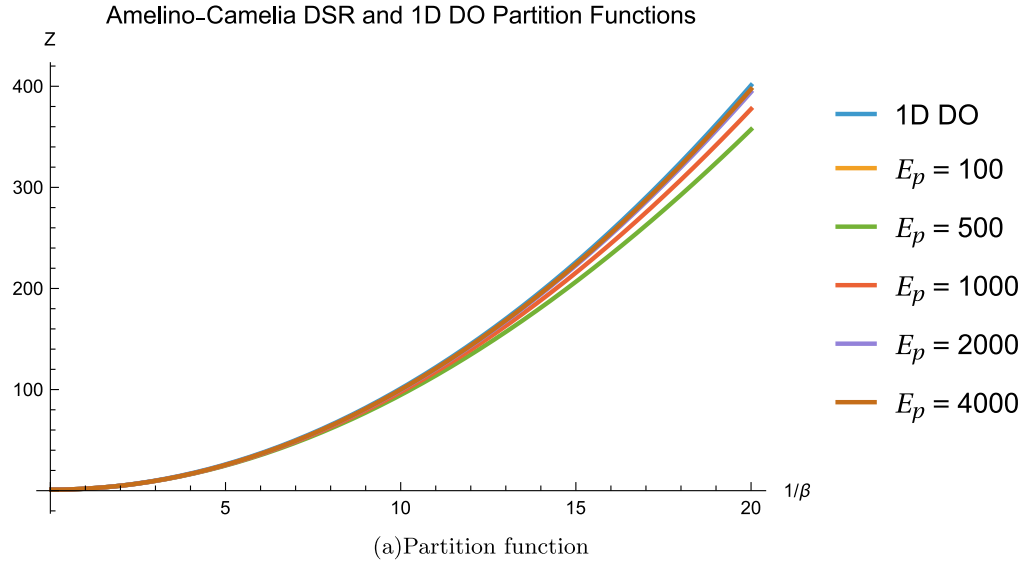

(a)Partition function

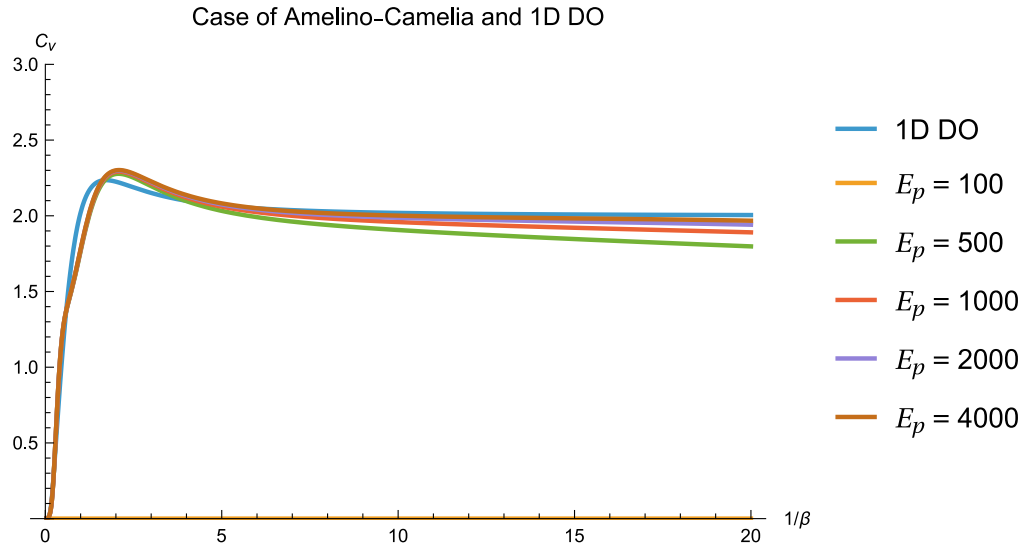

(b)Specific heat

Figure 1. The behavior of the partition function and specific heat of the one-dimensional Dirac oscillator (1D DO) as a function of $1/\beta$ in the framework of Amelino-Camelia DSR, and its comparison with the standard 1D DO.

fluctuations. Their representation as derivatives of the partition function unifies the study of diverse phenomena in various physical situations.

Prior to presenting numerical results, we emphasize that our analysis is restricted exclusively to stationary states characterized by positive energies. Two principal justifications underpin this decision [29]:

- The Dirac Oscillator (DO) inherently possesses an exact Foldy–Wouthuysen transformation (FWT) [30, 31], which cleanly separates solutions into positive- and negative-energy states. Consequently, thermodynamic calculations are exclusively associated with positive-energy states, thereby precluding particle–antiparticle annihilation or mixing with negative-energy states under this formalism.
- The approach assumes complete occupancy of all negative-energy states (antiparticles). Although traditionally associated with fermions through the concept of the Dirac sea, this concept is generalized here to bosons. Unlike fermions, bosons do not adhere to the Pauli exclusion principle and can simultaneously occupy identical negative-energy states [26, 32, 33].

Therefore, the fermionic spectrum naturally divides into two distinct branches: one comprising positive-energy states and the other negative-energy states. An effective energy barrier exists between these two branches, analogous to the bandgap observed in solid-state systems, effectively preventing transitions between them [25, 34].

Although the Dirac oscillator Hamiltonian belongs to a category of relativistic quantum systems defined by the stability of the Dirac sea, it distinctly separates positive and

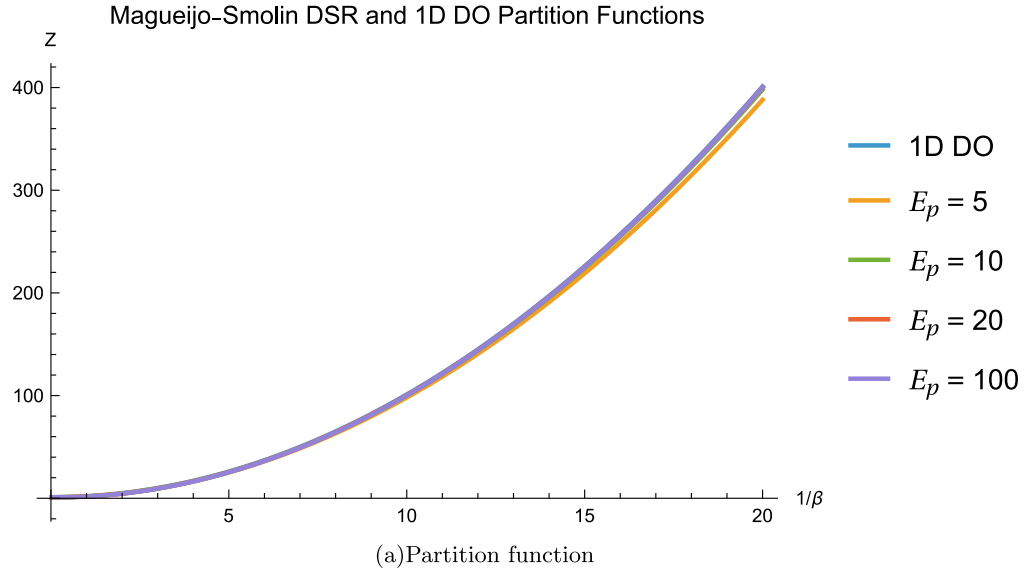

(a)Partition function

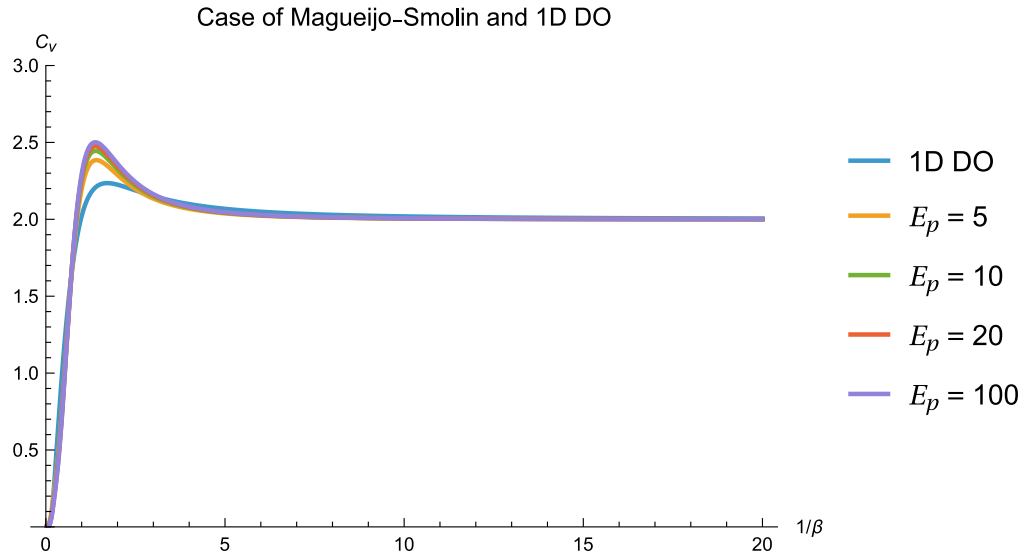

(b)Specific heat

Figure 2. The behavior of the partition function and specific heat of the one-dimensional DO (1D DO) as a function of $1/\beta$ in the framework of MS DSR, and its comparison with the standard 1D DO.

negative-energy solutions without intermixing. This characteristic is rigorously demonstrable via the Foldy–Wouthuysen canonical transformation. Nevertheless, it merits consideration whether negative-energy branches might also contribute to thermal properties. Myers *et al* [34] have advocated for including negative-energy states in thermal calculations, arguing their role as supersymmetric counterparts to positive-energy states. To our knowledge, this represents an innovative perspective within the literature. However, when applied to relativistic oscillators, such an approach results in an unintended doubling of the specific heat. More critically, in the non-relativistic regime, it yields values twice those empirically validated in solid-state physics, where thermal characteristics derived solely from positive-energy (electron) states exhibit excellent congruence with experimental observations.

In summary, this investigation addresses the thermodynamic properties of the one-dimensional Dirac Oscillator under the assumption that the positive-energy branch predominantly influences thermal behavior. Specifically, we analyze the partition function and specific heat associated exclusively with the positive-energy sector, aiming to clarify their impacts on the overall system dynamics.

Figure 1 illustrates the partition function and specific heat as functions of $1/\beta$ (where $\beta = 1/k_{\mathrm{B}}T$, with T the temperature) for the one-dimensional Dirac oscillator (1D DO) in the Amelino-Camelia DSR framework, compared to the standard 1D DO. The Amelino-Camelia DSR introduces a deformation at the Planck scale, which alters the oscillator's energy spectrum. This modification leads to notable deviations in the partition function and specific heat curves from the standard case, particularly at high temperatures

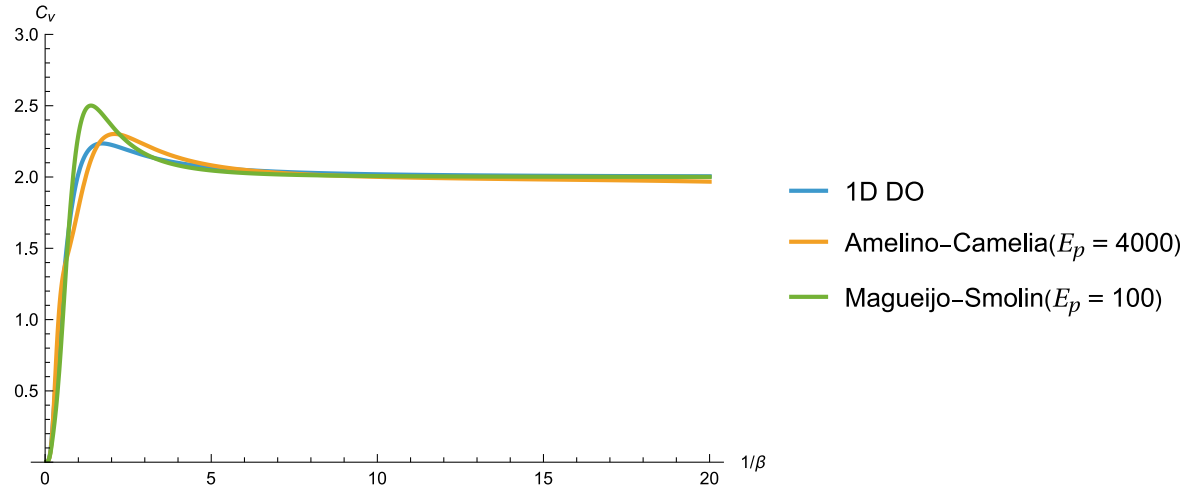

Figure 3. Comparison of the specific heat as a function of $1/\beta$ for the one-dimensional DO (1D DO) in the frameworks of Amelino-Camelia and MS DSR, with that of the standard 1D DO.

(corresponding to low β). These deviations arise because the DSR framework imposes an upper bound on the accessible energy states, suppressing or enhancing the thermodynamic quantities relative to the undeformed oscillator. At low temperatures (high β), all models converge, as the influence of quantum gravity effects diminishes. Thus, figure 1 demonstrates how Planck-scale physics, as encoded by Amelino-Camelia DSR, significantly modifies the thermodynamic behavior at high temperatures, with the most pronounced differences occurring near the Planck scale.

A vital feature displayed in this figure is the singularity of the modified energy spectrum: the denumerator $2E_p^2 - mn\omega$ vanishes with n tending to the critical number $n_c = 2E_p^2/(m\omega)$. When n approaches n_c, the energy blows up, and for $n > n_c$, the spectrum becomes unphysical (complex or singular). This singularity's presence, which is the hallmark of the Planck-scale deformation, restricts the number of excitations and hence the maximum amount of energy that can be paid to the system. In contrast to the standard 1D DO, where the energy levels are untruncated, the spectrum of the DSR-deformed oscillator is limited at n_c. This upper bound causes the partition function and specific heat to saturate or even suppress at large T, since states above the singularity will be disallowed to be thermally populated. This can be seen in the flattening or suppression of thermodynamic curves at high temperatures for the DSR case, as opposed to the continued rise exhibited by the standard DO. The bifurcation is a signpost for Planck-scale physics in the Amelino-Camelia DSR model, due to a fundamental energy spectrum cutoff that is missing from ordinary quantum mechanics and relativity.

For increasing deformation parameter E_p, the singularity is moved to infinity ($n_c \to \infty$) and the DSR spectrum continuously approaches the ordinary 1D DO one, $E_{\pm}(n) = \pm\sqrt{m^2 + 2nm\omega}$. However, for any finite E_p, the singularity is going to change the spectrum drastically, and thus, one can not ever hope to reproduce the standard oscillator at high energies exactly. This means that, practically, the DO deformation of the DSR-deformed DO is the same as that of the standard DO for small n (i.e., the low-energy limit), where the singularity is located away from us. At higher energies, DSR corrections become essential, and the singularity prevents the system from reaching the entire standard DO spectrum. Therefore, when E_p is finite, the accessible energy levels for the Dirac oscillator are bound from above by the quadratic potential, which has to have significant consequences on the microscopic (spectral) as well as on the macroscopic (thermodynamic) aspects.

Figure 2 displays the partition function and specific heat as functions of $1/\beta$ for the 1D DO in the MS DSR framework, alongside the standard oscillator for comparison. The MS DSR framework also modifies the energy-momentum relation, but with a different mathematical structure than Amelino-Camelia DSR. As a result, the partition function and specific heat curves diverge from the standard case at high temperatures. Still, the pattern and magnitude of the deviations are distinct from those in figure 1. Typically, the MS model leads to a stronger suppression of thermodynamic quantities at high temperatures, reflecting a more restrictive upper bound on energy states. Comparing figures 1 and 2 reveals the unique signatures of the two DSR models, underlining the importance of the specific form of Planck-scale deformation in determining observable thermodynamic effects.

Figure 3 offers a direct comparison of the specific heat as a function of $1/\beta$ for the 1D DO in both Amelino-Camelia and MS DSR frameworks, as well as the standard (undeformed) case. At low temperatures (high β), all curves overlap, indicating negligible DSR effects. As the temperature rises (lower β), both DSR models predict a suppression of specific heat relative to the standard case. Still, the onset and degree of suppression differ: the MS model typically shows the most substantial reduction at high temperatures, while the Amelino-Camelia model exhibits a milder, though still significant, deviation. This figure encapsulates the core finding that Planck-scale deformations in DSR frameworks lead to observable differences in thermodynamic properties, with specific heat serving as a sensitive probe of quantum

gravity effects. The distinct behaviors of the two DSR models underscore the potential for experimental discrimination between different quantum gravity scenarios.

In summary, these three figures collectively demonstrate how Amelino-Camelia and MS DSR models imprint distinct signatures on the thermal properties of the one-dimensional Dirac oscillator. The differences arise from the unique ways each DSR framework modifies the energy spectrum, leading to varying degrees of suppression in the partition function and specific heat at high temperatures. These visualizations offer clear, comparative insight into the phenomenological consequences of Planck-scale physics, highlighting the potential for using thermodynamic observables to test quantum gravity-inspired modifications of special relativity.

5. Conclusion

In this work, we derive and compare the energy spectra of the one-dimensional Dirac oscillator under two prominent DSR schemes—Amelino-Camelia and MS—obtaining analytic expressions in the leading Planck-scale deformation and verifying that both reproduce the standard relativistic oscillator levels as the DSR scale tends to infinity [1]. By inserting these spectra into the partition function and employing the Euler–Maclaurin expansion, we demonstrated that Planck-scale deformations impose an upper bound on accessible energy states, leading to a pronounced suppression and eventual saturation of thermodynamic quantities (partition function, internal energy, specific heat) at high temperatures compared to the undeformed case [1]. Our analysis reveals distinct signatures between the two DSR models: the MS framework typically yields stronger high-temperature suppression than the Amelino-Camelia prescription, offering a potential phenomenological discriminator in future experiments or simulations [1]. These findings highlight how DSR-induced modifications lead to observable deviations in the thermal behavior of relativistic quantum systems, and they pave the way for further studies on more complex potentials, higher-dimensional oscillators, and the incorporation of interactions beyond the single-particle level.

Acknowledgments

We are very grateful to the referee for the careful reading of the paper and for the detailed suggestions, which helped us to improve considerably.

NJ has been funded by the Science Committee of the Ministry of Science and Higher Education of the Republic of Kazakhstan, Program No. BR24992759.

References

[1] Ito D, Mori K and Carriere E 1967 An example of dynamical systems with linear trajectory *Il Nuovo Cimento A (1965–1970)* **51** 1119–21

[2] Moshinsky M and Szczepaniak A 1989 The Dirac oscillator *J. Phys. A: Math. Gen.* **22** L817

[3] Benítez J, Martínez y Romero R P, Núñez-Yépez H N and Salas-Brito A L 1990 Solution and hidden supersymmetry of a Dirac oscillator *Phys. Rev. Lett.* **64** 1643–6

[4] Quesne C and Moshinsky M 1990 Symmetry lie algebra of the Dirac oscillator *J. Phys. A: Math. Gen.* **23** 2263

[5] Quesne C and Tkachuk V M 2005 Dirac oscillator with nonzero minimal uncertainty in position *J. Phys. A: Math. Gen.* **38** 1747

[6] Boumali A 2015 The one-dimensional thermal properties for the relativistic harmonic oscillators *EJTP* **12** 1–10

[7] Quimbay C and Strange P 2013 Quantum phase transition in the chirality of the (2+1)-dimensional Dirac oscillator arXiv:1312.5251

[8] Franco-Villafane J A, Sadurni E, Barkhofen S, Kuhl U, Mortessagne F and Seligman T H 2013 First experimental realization of the Dirac oscillator *Phys. Rev. Lett.* **111** 170405

[9] Boumali A, Serdouk F and Dilmi S 2020 Superstatistical properties of the one-dimensional Dirac oscillator *Physica* A **553** 124207

[10] Guvendi A and Boumali A 2021 Superstatistical properties of a fermion–antifermion pair interacting via Dirac oscillator coupling in one-dimension *The European Physical Journal Plus* **136** 1–18

[11] Pacheco M H, Landim R R and Almeida C A S 2003 One-dimensional Dirac oscillator in a thermal bath *Phys. Lett.* A **311** 93–6

[12] Pacheco M H, Maluf R V, Almeida C A S and Landim R R 2014 Three-dimensional dirac oscillator in a thermal bath *Europhys. Lett.* **108** 10005

[13] Siouane S and Boumali A 2024 On the superstatistical properties of the Klein–Gordon oscillator using gamma, log, and F distributions *J. Low Temp. Phys.* **217** 598–617

[14] Siouane S, Boumali A and Guvendi A 2024 Superstatistical properties of the Dirac oscillator with gamma, lognormal, and F distributions *Theor. Math Phys.* **219** 673–87

[15] Amelino-Camelia G 2002 Testable scenario for relativity with minimum-length *Int. J. Mod. Phys.* D **11** 35–60

[16] Amelino-Camelia G 2002 Relativity in spacetimes with short-distance structure governed by an observer-independent (Planckian) length scale *Int. J. Mod. Phys.* D **11** 1643

[17] Magueijo J and Smolin L 2002 Lorentz invariance with an invariant energy scale *Phys. Rev. Lett.* **88** 190403

[18] Jafari N and Shariati A 2011 Projective interpretation of some doubly special relativity theories *Phys. Rev.* D **84** 065038

[19] Jafari N and Guvendi A 2020 Dispersion relations in finite-boost DSR *Phys. Lett.* B **809** 135735

[20] Shukirgaliyev B and Jafari N 2024 Nonrelativistic limits of the Klein–Gordon and Dirac equations in the Amelino–Camelia DSR *Phys. Lett.* B **853** 138693

[21] Jafari N and Guvendi A 2025 Two-body Dirac equation in DSR: results for fermion-antifermion pairs *Phys. Lett.* B **866** 139515

[22] Guvendi A, Mustafa O and Jafari N 2025 Amelino-Camelia DSR effects on charged Dirac oscillators: modulated spinning magnetic vortices *Phys. Lett.* B **866** 139547

[23] Coraddu M and Mignemi S 2010 The nonrelativistic limit of the Magueijo–Smolin model of deformed special relativity *Europhys. Lett.* **91** 51002

[24] Boumali A 2015 Thermodynamic properties of the graphene in a magnetic field via the two-dimensional Dirac oscillator *Phys. Scr.* **90** 045702

[25] Boumali A and Hassanabadi H 2015 Exact solutions of the (2+1)-dimensional Dirac oscillator under a magnetic field in the presence of a minimal length in the non-commutative phase space *Zeitschrift für Naturforschung* A **70** 619–27

[26] Boumali A 2015 Thermal properties of the one-dimensional Duffin–Kemmer–Petiau oscillator using Hurwitz zeta function *Zeitschrift für Naturforschung* A **70** 867–74
[27] Andrews G, Askey R and Roy R 1999 *Special Functions* (Cambridge University Press)
[28] Elliot D 1998 The Euler–Maclaurin formula revisited *J. Aust. Math. Soc.* **40** E27
[29] Boumali A 2015 Exact solutions of the (2+1)-dimensional Dirac oscillator in the presence of a minimal length *Z. Nat. forsch.* **70** 867
[30] Foldy L L and Wouthuysen S A 1950 On the dirac theory of spin 1/2 particles and its non-relativistic limit *Phys. Rev.* **78** 29–36
[31] Foldy L L and Wouthuysen S A 1952 The electromagnetic properties of Dirac particles *Phys. Rev.* **87** 688–93
[32] Nielsen H B and Ninomiya M 2005 Dirac sea for bosons: 1. Formulation of negative energy sea for bosons *Prog. Theor. Phys.* **113** 603
[33] Nielsen H B and Ninomiya M 2005 Dirac sea for bosons: ii. Study of the naive vacuum theory for the toy model world prior to filling the negative energy sea *Prog. Theor. Phys.* **113** 625
[34] Myers N M, Abah O and Deffner S 2021 Quantum otto engines at relativistic energies *New J. Phys.* **23** 105001